



A novel agonist with homobivalent single-domain antibodies that bind the FGF receptor 1 domain III functions as an FGF2 ligand

Received for publication, July 1, 2022, and in revised form, October 21, 2022. Published, Papers in Press, December 15, 2022,

<https://doi.org/10.1016/j.jbc.2022.102804>

Ryo Yonehara^{1,*,#}, Shigefumi Kumachi^{1,#}, Kenji Kashiwagi^{2,#}, Kanako Wakabayashi-Nakao^{1,#}, Maiko Motohashi¹, Taihei Murakami¹, Teruhiko Yanagisawa², Hidenao Arai¹, Akikazu Murakami³ , Yukio Ueno², Naoto Nemoto¹, and Masayuki Tsuchiya^{1,*}

From the ¹Epsilon Molecular Engineering, Inc, Saitama, Japan; ²Sekisui Chemical Co, Ltd, Tokyo, Japan; ³RePHAGEN Co, Ltd, Uruma, Japan

Edited by Donita Brady

Fibroblast growth factor (FGF) is a multifunctional protein that exhibits a wide range of biological effects. Most commonly, it acts as a mitogen, but it also has regulatory, morphological, and endocrine effects. The four receptor subtypes of FGF are activated by more than 20 different FGF ligands. FGF2, one of the FGF ligands, is an essential factor for cell culture in stem cells for regenerative medicine; however, recombinant FGF2 is extremely unstable. Here, we successfully generated homobivalent agonistic single-domain antibodies (variable domain of heavy chain of heavy chain antibodies referred to as VHs) that bind to domain III and induce activation of the FGF receptor 1 and thus transduce intracellular signaling. This agonistic VHH has similar biological activity (EC_{50}) as the natural FGF2 ligand. Furthermore, we determined that the agonistic VHH could support the proliferation of human-induced pluripotent stem cells (PSCs) and human mesenchymal stem cells, which are PSCs for regenerative medicine. In addition, the agonistic VHH could maintain the ability of mesenchymal stem cells to differentiate into adipocytes or osteocytes, indicating that it could maintain the properties of PSCs. These results suggest that the VHH agonist may function as an FGF2 mimetic in cell preparation of stem cells for regenerative medicine with better cost effectiveness.

Broad-spectrum mitogens, such as fibroblast growth factors (FGFs), by definition, play a role in a variety of cellular functions that include migration, proliferation, differentiation, and survival. Furthermore, FGFs potently induce differentiation and proliferation against various tissue-specific stem cells including bone marrow-derived mesenchymal, hematopoietic, neural, spermatogonial, and prostate (1–3). Some FGF family members (FGF2, FGF4, FGF6, FGF7, FGF8, and FGF9) reportedly affect the stemness of pluripotent stem cells (PSCs). Among them, FGF2 and FGF4 have been clearly demonstrated to be highly pertinent in maintaining mouse and human stem

cells in the undifferentiated state. Although human-induced pluripotent stem cells (hiPSCs) express all four FGF receptors (FGFRs), it has been reported that the binding of FGF2 to FGFR1, considered the most important receptor, activates downstream signaling including mitogen-activated protein kinases (Ras/Raf–MEK–MAPKs), PI3K/protein kinase B (PI3K/AKT), PLC γ , and the signal transducer and activator of the transcription pathway (1, 4, 5). That is, FGF2 is mandatory for restraining the pluripotency state of hiPSCs (6) and human embryonic stem cells (ESCs) (7, 8).

With the establishment of culture methods for ESCs and the discovery of iPSCs in the past few decades, there has been a growing need for synthetic alternatives to FGF2. Although considered quite useful, recombinant FGF2 has low thermal stability and shows inconsistency between batches that may reduce the integrity of the stem cell culture. The high cost of production has restrained the scalability of stem cell culture and so, basic research in stem cell-based regenerative therapy is not robust. Synthetic alternatives for FGF2, therefore, are of importance in stem cell-based regenerative medicines (8).

One approach has been to generate artificial agonists of FGFR1. The FGFR gene family includes FGFR1, FGFR2, FGFR3, and FGFR4. It is known that FGFR1, FGFR2, and FGFR3 generate alternative splicing variants of immunoglobulin-like domain III (IIIb and IIIc) that are important in the determination of ligand-binding specificity. FGF2 binds to FGFR1, helped by heparin or heparan sulfate proteoglycans for the induction of dimerization, leading to the phosphorylation of FGFR1. Therefore, most FGFR1 agonists have been designed to induce dimerization of FGFR1. At this time, none of them have been used as an alternative for FGF2 because of low efficacy. It may be that these artificial agonists, compared with native ligands, do not mimic the mode of dimerization or induce the activation of the receptor. Another approach is to use DNA aptamers that act as functional mimics of FGF2 (9). The most potent aptamer assemblies (dimers) are composed of two single-stranded DNAs and could support the self-renewal and pluripotency of iPSCs. However, this failed to sustain long-term maintenance of stem cells.

[#] These authors contributed equally to this work.

* For correspondence: Ryo Yonehara, yonehara@epsilon-mol.co.jp; Masayuki Tsuchiya, tsuchiya@epsilon-mol.co.jp.

A novel agonist for FGFR1 functions as FGF2 ligand

Single-domain antibodies, VHHs (variable domain of heavy chain of heavy chain antibodies), are minimal and monomeric antigen-binding domains derived from camelid single-chain antibodies (10). VHHs are highly soluble, stable, readily constructed into multivalent formats, and amenable to low cost and efficient bacterial production. Herein, we report homobivalent VHHs that can induce FGFR1 dimerization and thereby activate downstream MAPK/extracellular signal-regulated protein kinase (ERK) signaling pathways. Anti-FGFR1 VHHs, isolated from a coupled screening (complementary DNA [cDNA] display (11–15) and phage display), exhibited a high affinity of binding to FGFR1 with dissociation constants (K_D) ranging from 1 to 2 nM. Concerning thermal stability, the VHHs we obtained showed a T_m value as high as 77.9 °C. Although the monovalent VHHs do not activate intracellular (IC) signaling such as the MAPK/ERK signaling pathway, they result in effective agonist activity by producing homobivalent VHHs with various linkers such as the GSGGG linker. We further demonstrate that homobivalent VHHs have stronger biological activity than FGF2, suggesting that they merit further investigation as a promising candidate for cellular response. As far as we know, our homobivalent VHHs are the first example of agonist antibodies based on VHHs, opening a new opportunity to generate artificial agonists for various receptors.

Results

Isolation of VHHs against FGFR1 extracellular domain

The cDNA display technique enables *in vitro* selection to identify the various kinds of binders from large naïve VHH libraries, currently over 10^{13} in size; it was difficult to choose the strongest binder with cDNA display alone. On the other hand, the phage display is a powerful tool for selecting binders that bind with high affinity and specificity to target molecules under stringent condition. As shown in Figure 1A, we carried out a coupled screening with both cDNA and phage displays to isolate high-affinity binders. First, binders against a soluble FGFR1 extracellular domain (FGFR1 ED) were selected after the fourth-round screening from the initial VHH cDNA display library with a diversity of 10^{13} clones. The VHH genes from the pool of binders from the cDNA display were PCR amplified and then transferred into a phagemid vector. Phage display panning was then performed twice to select high-affinity binders. The phage ELISA at each panning was performed to guarantee the presence of the binders. The ELISA data indicated that the pooled phage mixture contained positive clones (Fig. 1B). Next, to select positive single clones from the mixture, the binders were further subjected to selection, and 13 of the 15 clones clearly did bind to the antigen (Fig. 1C).

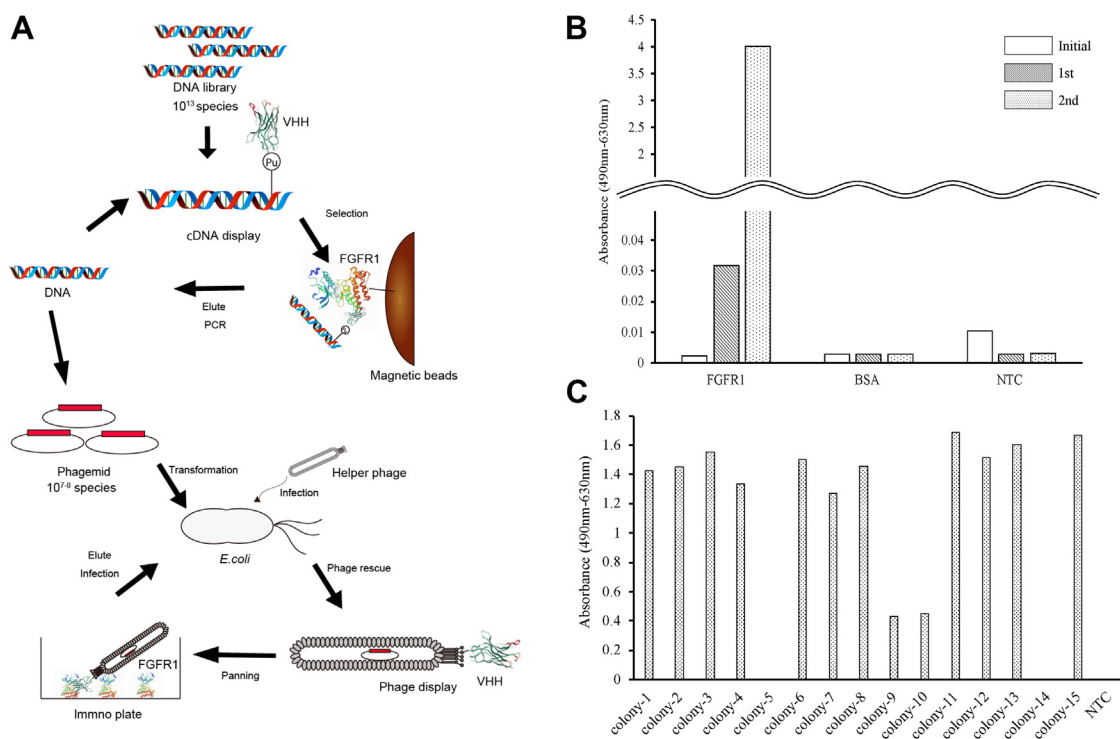


Figure 1. Successive screening and phage ELISA. A, schematic diagram of a coupled successive screening method with two technologies (cDNA display and phage display). The cDNA display VHH library was synthesized from the DNA of the initial VHH library. The cDNA display library was mixed with an antigen FGFR1 immobilized on magnetic beads. After washing the beads, the binders were eluted and their cDNA sequences determined after PCR amplification. The PCR-amplified VHH cDNAs were transferred to a phagemid vector. The phagemid vector was electroporated into the *Escherichia coli*, and then the helper phage was infected. The phages produced were collected from the supernatant. This phage display library was mixed with an antigen FGFR1 immobilized on an immune plate. After washing the plates, the binders were eluted and infected with *E. coli* for the next panning cycle. B, phage ELISA was performed for the pooled phages from the initial, second, and third round phage display libraries. C, phage ELISA was performed for each of the 15 candidates from the third round phage display. cDNA, complementary DNA; FGFR1, fibroblast growth factor receptor 1; VHH, variable domain of heavy chain of heavy chain antibody.

Characterization of VHHs

DNA sequence analyses of the 15 selected clones (Fig. 1C) showed that two were unique clones with similar complementarity-determining region 3 (CDR3) sequences. To confirm binding activities to FGFR1 ED, colony 1 and colony 9, thereafter designated as clone VM34 and clone VM35 (Fig. S1A), respectively, were inserted into an expression vector in *Corynebacterium glutamicum*. Next, clone VM34 and clone

VM35 were subsequently expressed and purified from a culture medium (Fig. S1, B and C). The FGFR1 (IIIc)-Fc was immobilized onto a Biacore sensor chip, and the binding activities were determined. Clone VM34 and clone VM35 bound to the target with a K_D of 1.74 and 1.02 nM, respectively (Fig. 2A and Table 1). Furthermore, a competition binding assay suggested that both clone VM34 and clone VM35 bound to a similar region (Fig. 2B). This result was consistent with a high similarity

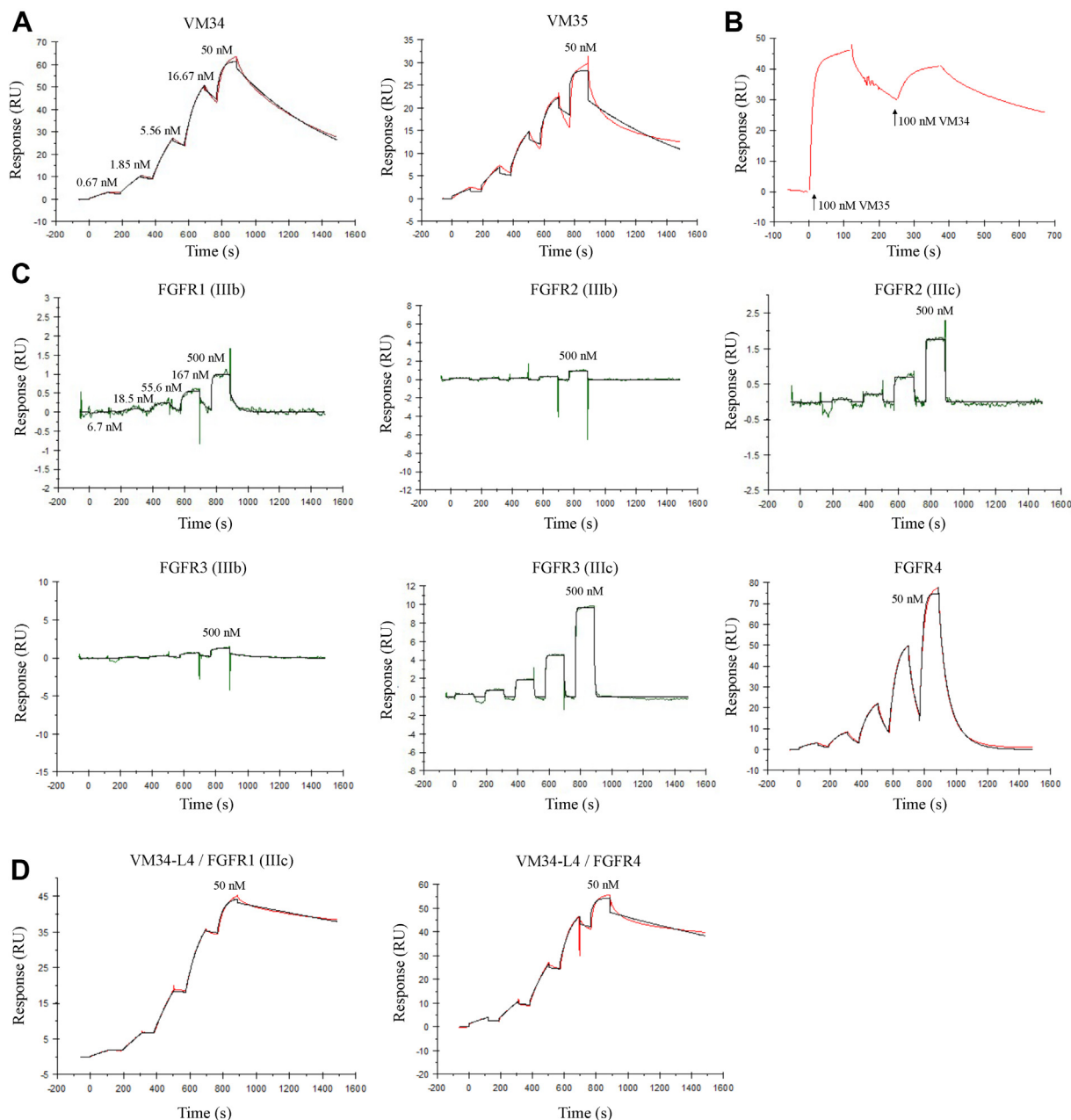


Figure 2. Binding analysis of VHHs. A, the binding activities of monovalent clones VM34 and VM35 against FGFR1 ED were confirmed by immobilizing FGFR1(IIIc)-Fc to a Biacore T200 sensor chip (Cytiva). B, monovalent clones VM34 and VM35 were subjected to a competitive binding inhibition analysis of the FGFR1 ED using the Biacore T200 system. The biotinylated recombinant FGFR1 ED was immobilized on a Biotin CAPture chip, yielding typical levels of approximately 250 RUs. Then, VM35 was injected at 100 nM at a flow rate of 30 μ l/min for 120 s. VM34 was sequentially injected for 120 s. The values of maximum RU for VM35 reached approximately 50 RUs. On the other hand, the values of maximum RU for VM34 injected sequentially reached approximately 40 RUs, suggesting that VM35 inhibited the binding of VM34; thus, VM34 and VM35 bound to the same region of the FGFR1 ED. C, the binding characteristics of monovalent clone VM34 against FGFR1 (IIIb), FGFR2 (IIIb), FGFR2 (IIIc), FGFR3 (IIIb), FGFR3 (IIIc), and FGFR4 were measured using a Biacore T200 system. D, the binding characteristics of homobivalent VM34-L4 against FGFR1(IIIc) (left) and FGFR4 (right) were measured using a Biacore T200 system. FGFR1 ED, FGFR1 extracellular domain; VHH, variable domain of heavy chain of heavy chain antibody.

A novel agonist for FGFR1 functions as FGF2 ligand

Table 1
SPR analysis of binding kinetics of VM34 and VM35 for each receptor

Receptor	VM34			VM35		
	k_{on} (1/Ms)	k_{off} (1/s)	K_D (M)	k_{on} (1/Ms)	k_{off} (1/s)	K_D (M)
FGFR1 (IIIb)	2.74×10^5	2.54×10^{-2}	9.28×10^{-8}	Not determined		
FGFR1 (IIIc)	8.19×10^5	1.42×10^{-3}	1.74×10^{-9}	1.11×10^6	1.14×10^{-3}	1.02×10^{-9}
FGFR2 (IIIb)	No binding			Not determined		
FGFR2 (IIIc)	4.84×10^5	7.76×10^{-1}	1.60×10^{-6}	Not determined		
FGFR3 (IIIb)	No binding			Not determined		
FGFR3 (IIIc)	2.32×10^5	2.35×10^{-1}	1.01×10^{-6}	Not determined		
FGFR4	2.37×10^6	5.27×10^{-2}	2.22×10^{-8}	Not determined		

between the CDR3 sequences from clone VM34 and clone VM35. Briefly, the amino-acid residues of VM34 in CDR3 (S98–Y104, Y106–P109, and G111–V114) are the same as those of VM35, whereas only two residues are different from each other: L105 and G110 differ from VM34; Y105 and Q110 differ from VM35 (Fig. S1A). The thermal stability analysis of the differential scanning fluorimetry (DSF) measurements revealed that clone VM34 has a higher T_m (Table 2), suggesting it should be suitable as a protein engineering candidate for FGFR1 agonist.

Binding specificity and binding region of VHH for FGFRs

The FGFR gene family is comprised of four members—FGFR1, FGFR2, FGFR3, and FGFR4. Among them, FGFR1, FGFR2, and FGFR3 generate two major splice variants in the immunoglobulin-like domain III, referred to as IIIb and IIIc. The surface plasmon resonance (SPR) analysis revealed that the binding affinity of clone VM34 for FGFR1 (IIIb) was lower than that for FGFR1 (IIIc) and that clone VM34 bound to the FGFR2 (IIIc) and FGFR3 (IIIc) but did not bind to their splicing variants FGFR2 (IIIb) and FGFR3 (IIIb). The dissociation rates of clone VM34 for FGFR1 (IIIb), FGFR2 (IIIc), and FGFR3 (IIIc) were significantly faster, resulting in a decrease in the binding affinity for each FGFR (Fig. 2C and Table 1). These results indicate that the IIIc region in domain III contains the binding site. Furthermore, the sequence alignment and structural comparison of domain III from FGFR1 (IIIc), FGFR2 (IIIc), and FGFR3 (IIIc) show that the IIIc region is conserved among these receptors, resulting in the different areas that are the potential binding epitope for VM34: region I, II, or III (Figs. S2 and S3).

We also analyzed the binding affinity for FGFR4. The SPR experiments revealed that clone VM34 associates and dissociates faster with FGFR4 than with FGFR1 (IIIc) (Fig. 2C and Table 1). This result is consistent with the higher sequence

Table 2
Thermal stabilities of VHHs

VHHs	T_m (°C)	$T_{\text{agg}266}$ (°C)
Clone VM34	77.9	46.1
Clone VM35	74.7	50.2
Clone VM34-5aa	81.0	34.3
Clone VM34-10aa	78.3	37.5
Clone VM34-20aa	85.3	64.1
Clone VM34-L3	80.7	44.3
Clone VM34-L4	82.3	50.0

similarity between domain III of FGFR1 (IIIc) and FGFR4 (Fig. S3A).

Construction and characterization of homobivalent VHHs

The optical length of dimerization on FGFR1 by FGF2 is important for its activation (16). Therefore, we generated homobivalent VHHs linked with various lengths: 5aa, 10aa, 20aa, L3, and L4. The 5aa, 10aa, and 20aa consisted of a C- to N-terminal fusion of clone VM34 or clone VM35 via a 5-, 10-, or 20-amino acid Gly-Ser linker, respectively, whereas the L3 and L4 consisted of another flexible linker (Fig. S1, B and C). The SPR experiments showed that the homobivalent VHHs have 20- to 40-fold higher affinity to FGFR1 (IIIc) than monovalent VHHs (Fig. 2D and Table 3). Next, using DSF and static light scattering (SLS) techniques, we characterized the biophysical properties of these homobivalent VHHs. These homobivalent VHHs exhibited good thermal stabilities (Table 2).

Effect of VHHs on the FGFR-mediated signaling pathways and cell growth

To get more insight into those VHHs, we investigated the effect of VHH binding to FGFR on the signaling pathway in NIH3T3 mouse fibroblast cells and its proliferation. The FGF2 ligand binds to FGFR mediated by heparin sulfate proteoglycans on the cell surface and then induces structural changes in FGFR dimers leading to activation of the IC signaling pathways, such as MAPKs. Erk1/2 are activated by MAPK factors and associated with growth, differentiation and proliferation. As shown in Figure 3, FGF2 induced the phosphorylation of Erk1/2. The monovalent clone VM34 did not induce the phosphorylation of Erk1/2, whereas VM35 showed weak activity (Fig. S4). These results suggest that it is difficult to activate FGFR1 by using monovalent VHHs. On the other hand, homobivalent VHHs activated the Erk1/2 phosphorylation, such as the natural ligand FGF2 (Fig. 3A). Furthermore, the homobivalent clone VM34 stimulated cell proliferation, with an EC_{50} value stronger than that of FGF2 (340–440 pM versus 470 pM, respectively); whereas the homobivalent clone VM35 showed weaker growth potential for NIH3T3, suggesting that it is important to select the suitable clone for generating the VHH agonist (Fig. 3, B and C).

Effect of VHHs on the FGFR-mediated human mesenchymal stem cells and hiPSCs

Next, we investigated the maintenance of undifferentiated state on human mesenchymal stem cells (hMSCs). Both the

Table 3
SPR analysis of binding kinetics of homobivalent VM34 for FGFR1 (IIIc) and FGFR4

VHHs	FGFR1(IIIc)			FGFR4		
	k_{on} (1/Ms)	k_{off} (1/s)	K_D (M)	k_{on} (1/Ms)	k_{off} (1/s)	K_D (M)
VM34-5aa	4.62×10^5	2.69×10^{-4}	5.82×10^{-10}	7.61×10^5	4.81×10^{-4}	6.31×10^{-10}
VM34-10aa	4.75×10^5	2.44×10^{-4}	5.13×10^{-10}	7.84×10^5	4.35×10^{-3}	5.55×10^{-10}
VM34-20aa	3.21×10^5	2.03×10^{-4}	6.32×10^{-10}	6.68×10^5	3.83×10^{-4}	5.73×10^{-10}
VM34-L3	3.20×10^5	2.25×10^{-4}	7.05×10^{-10}	5.46×10^5	4.14×10^{-4}	7.58×10^{-10}
VM34-L4	5.84×10^5	2.17×10^{-4}	3.72×10^{-10}	8.68×10^5	3.87×10^{-4}	4.46×10^{-10}

FGF2 ligand and the homobivalent VHH agonists could maintain cell proliferation ability for 25 days and induce no change in cell morphology (Fig. 4A). Cell surface marker analysis by flow cytometry showed that the cells cultured with medium containing FGF2 or homobivalent VHH agonist were positive for CD90, CD105, and CD73, which corresponds to the definition of MSCs according to the International Society for Cellular Therapy (Fig. 4B). hMSCs, somatic stem cells, are present in a wide range of tissues, such as bone marrow, adipose tissue, placenta, umbilical cord, and pulp. Depending on the culture conditions, the cells can differentiate into various

strains, such as osteoblasts, adipocytes, or chondrocytes. Here, we tested differentiation ability into adipocytes or osteoblasts of hMSCs. hMSCs maintained either with the FGF2 ligand or the homobivalent VHH agonist equally differentiated into adipocytes and osteoblasts, both types of cells (Fig. 4, C and D), suggesting that the homobivalent VHHs have the potential to act as useful and artificial alternatives to recombinant FGF2.

Finally, we assessed the effect of the expansion ability of a human iPS cell line, 253G1. Every 7 days, cell aggregates were disassembled into single cells, reseeded into 6-well plates, and cultured in medium containing FGF2 ligand or the

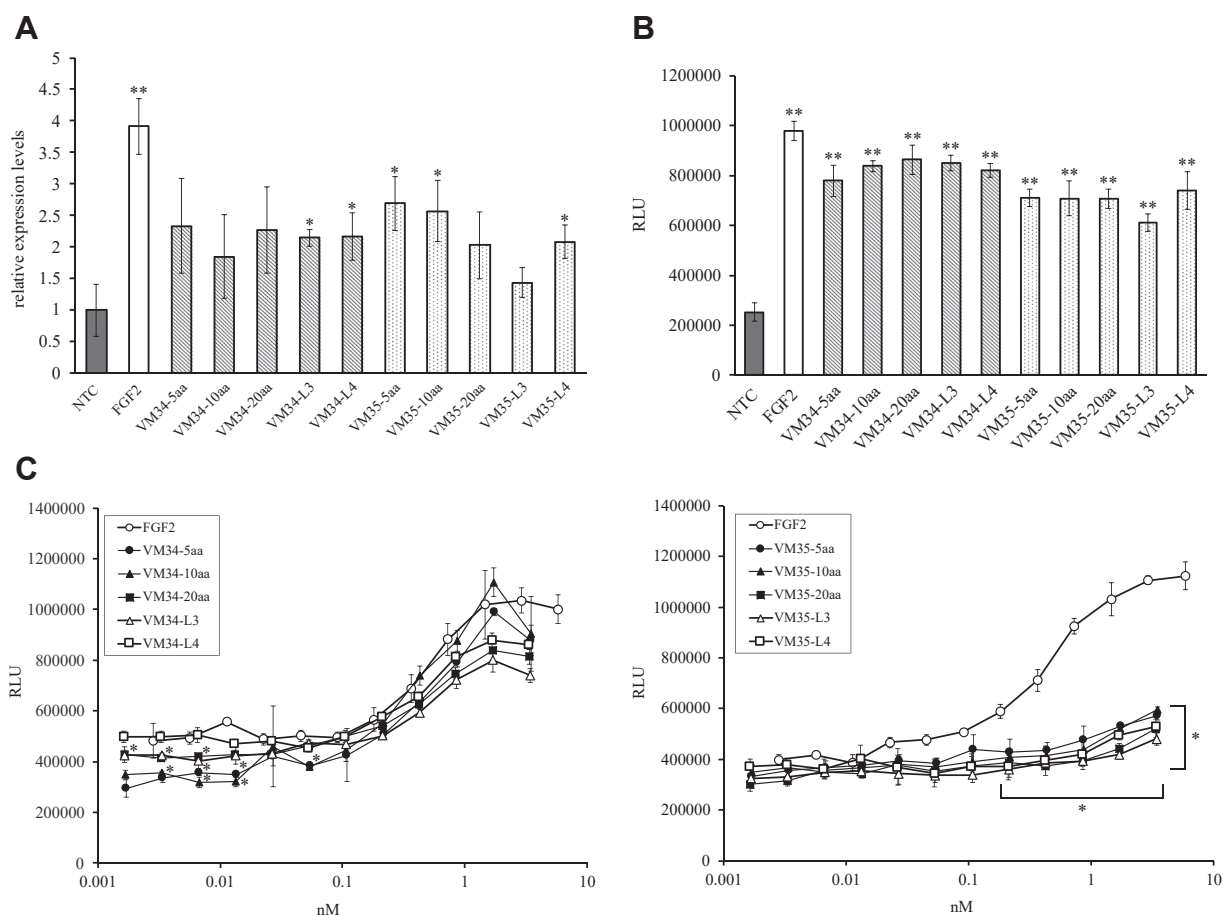


Figure 3. Agonistic activity of homobivalent VHHs on NIH3T3 cells. A, induction of Erk1/2 phosphorylation in NIH3T3 cells with FGF2 or VHHs. Cells were treated with FGF2 and homobivalent VHHs. The expression levels of phospho-Erk1/2 detected by in-cell ELISA. B, effect of cell proliferation in NIH3T3 cells treated with FGF2 and homobivalent VHHs. Cells were incubated in serum-free culture medium containing FGF2 or homobivalent VHH for 48 h; the number of viable cells was measured using a CellTiter-Glo 2.0 assay kit. Statistical significance was evaluated by Student's *t* test (**p* < 0.05, ** < 0.01 as compared with NTC) in (A) and (B). C, dose–response curves of homobivalent VHHs (left, clone VM34; right, clone VM35) and EC₅₀ values were also determined. All data are means ± SD of triplicate experiments. The homobivalent VHHs from VM34 have a higher agonistic activity than that from VM35. Statistical significance was evaluated by Student's *t* test (***p* < 0.01 as compared with FGF2) in (C). Erk1/2, extracellular signal–regulated protein kinase 1/2; FGF2, fibroblast growth factor 2; VHH, variable domain of heavy chain of heavy chain antibody.

A novel agonist for FGF receptor 1 functions as FGF2 ligand

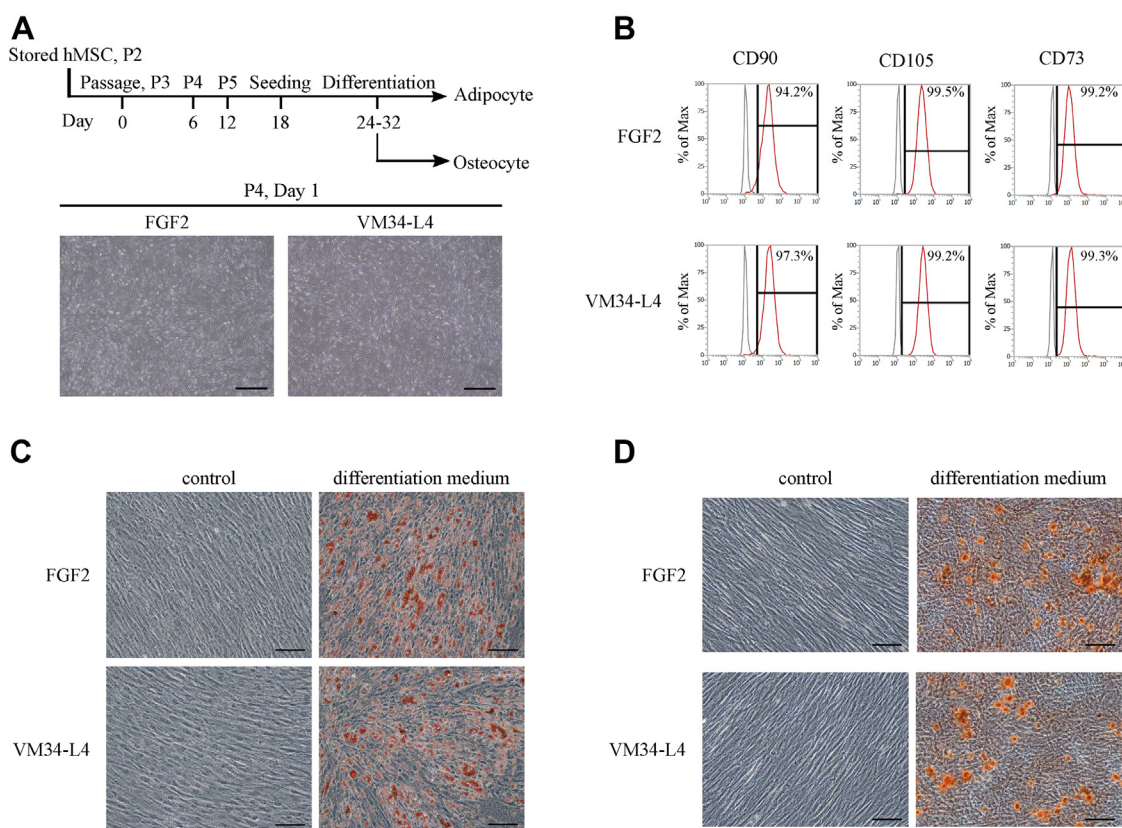


Figure 4. Homobivalent VHH and FGF2 stimulated cellular growth of hMSC under keeping undifferentiation potential. *A*, schematic diagram for the differentiation of hMSC into adipocyte and osteocyte (*up*). Phase contrast images of hMSC after passage 4 and day 5 of culture (*down*). *B*, flow cytometry analysis of hMSC cell-surface markers (CD90, CD105, and CD73) after 5 days of culture in FGF2- or homobivalent VHH medium. Curves in red show the specific markers, and curves in gray correspond to controls. *C*, comparison of adipogenic differentiation in hMSC passaging with FGF2- or homobivalent VHH medium by Oil Red O staining. The cells were incubated with control or differentiation medium for 8 days and stained with Oil Red O. The staining of control (*left*) and differentiated hMSC (*right*) was presented. *D*, comparison of osteogenic differentiation in hMSC passaging with FGF2- or homobivalent VHH medium by Alizarin Red staining. The cells were incubated with control or differentiation medium for 8 days and stained with Alizarin Red. The staining of control (*left*) and differentiated hMSC (*right*) was presented. All scale bars represent 500 μm . FGF2, fibroblast growth factor 2; hMSC, human mesenchymal stem cell; VHH, variable domain of heavy chain of heavy chain antibody.

homobivalent VHH. As shown in Fig. S5A, the cell number increased by approximately 10,000,000-fold over 28 days. Furthermore, the FGF2 ligand and the homobivalent VHH agonist could induce cell proliferation with no change in cell morphology (Fig. S5B). After long-term expansion culture, most cells were positive for OCT4 and SSEA4 (Fig. S5C). These results suggest that the homobivalent VHH agonist can maintain the undifferentiated state of 253G1 for long-term culture.

Discussion

A 26-residue peptide identified by phage display has been reported to be an artificial alternative to FGF2 (17). This peptide was found to specifically bind to the FGFR1c ED but showed no FGF ligand homology. Ballinger *et al.* (17) fused this polypeptide with the c-Jun leucine zipper domain that binds heparin and forms homodimers and found it specifically reproduced, with the same potency, the mitogenic and morphogenic activities of FGF2. For this activity, interaction with heparin was necessary, which illustrates the importance of heparin for FGFR activation even with ligands unrelated to

the FGF structure. Ueki *et al.* (9) reported using a DNA aptamer in the maintenance of iPSCs and showed that the DNA aptamer mimics the basic fibroblast growth factor (bFGF or FGF2). The most potent aptamer assembly (named TD0) consisting only of 76-mer single-stranded DNA may possibly support the self-renewal and pluripotency of iPSCs. However, the protocol for long-term culture using TD0 was found to be unable to sustain the expression of pluripotent markers in hiPSCs, indicating that the agonists may not concisely mimic the pattern of activation of IC signaling induced by bFGF.

Here, FGFR1 is most abundantly expressed in several human ESC lines and thus was selected for the target molecule. Natural FGF ligands are extremely unstable, which is a clinical obstacle. Therefore, we attempted to create a VHH-based agonist with exceptional structural and thermal stabilities. Both VHHs, clone VM34 and clone VM35, exhibited excellent thermal stability with a T_m of 77.9 and 74.7 $^{\circ}\text{C}$, respectively. The binding affinity studies were conducted mainly with clone VM34, which has the same binding epitope on FGFR1 as clone VM35 but has better thermal stability.

The binding characteristics against various receptors were analyzed (Table 1). Clone VM34 bound to both splice variants

of FGFR1, IIIb and IIIc and bound to FGFR2 (IIIc) and FGFR3 (IIIc). Members of the FGF family including FGF2, FGF4, FGF6, FGF7, FGF8, and FGF9 have been reported to impact the stemness of PSCs. The multiple signals from FGF/FGFR may provide some benefit. However, the value of binding activities to FGFR2 (IIIc) and FGFR3 (IIIc) was about 1000 times lower than to FGFR1 (IIIc). Therefore, it is doubtful whether it functions on target cells under physiological conditions, and thus we are awaiting future evaluation. Importantly, clone VM34 also has a high affinity to FGFR4 and is expected to give an advantageous effect because it has been clearly demonstrated that FGF2 and FGF4 are highly pertinent to maintain mouse and human stem cells in the undifferentiated state. Based on the binding properties to FGFRs, the sequence alignments, and the structural comparisons, the binding site of a VHH can be predicted to be on domain III (Fig. S3B).

Recently, an activation model of FGFR1 has been proposed according to the crystal structure of the FGFR1 ED–FGF2–heparin complex and quantitative imaging-FRET methodology (18, 19). In this model, FGFR1 is mainly monomeric under physiological conditions, and the binding of FGF2 induces its dimerization and activation because of the structural changes of the transmembrane and IC domains. Our binding analysis revealed that clone VM34 and clone VM35 bind to domain III on FGFR1 (Figs. 2 and S3); the functional assay showed that the homobivalent VHHs induces the phosphorylation of Erk1/2, the cell proliferation, and the maintenance of undifferentiated state on PSCs (Figs. 3, 4, and S5). These results suggest that, in the activation model, the homobivalent VHH connects to domain III, and that the structural changes of the transmembrane and IC domains cause an increase in the phosphorylation activity of FGFR1, resulting in proliferation of undifferentiated PSCs (Fig. 5).

Most importantly, the successive screening procedure can be applied to the selection of high-affinity VHHs. Indeed, the recent results in our laboratory indicate that high-affinity VHHs against various targets can be obtained using similar screening strategies described herein (data not shown). Furthermore, the methodologies of engineering applied to VHHs are applicable for the generation of artificial agonists because VHHs have size suitable for inducing agonist effects against EDs of receptors on a cell, which are smaller than immunoglobulin G (IgG) and larger than peptides.

Experimental procedures

Preparation of the cDNA display VHH library

An alpaca-derived VHH cDNA display library was prepared according to previous methods (15). Briefly, the alpaca-derived VHH cDNA library was provided by Dr Murakami at RePHAGEN, Inc. The DNA fragments for the cDNA display, composed of 5' UTR (T7 promoter, omega [Ω] enhancer, and Kozak consensus sequence), VHH gene, His-tag region, and 3' UTR linker hybridization region were transcribed and photocrosslinked with the 3-cyanovinylcarbazole nucleoside (cnvK) puromycin linker (20). The photocrosslinked product was

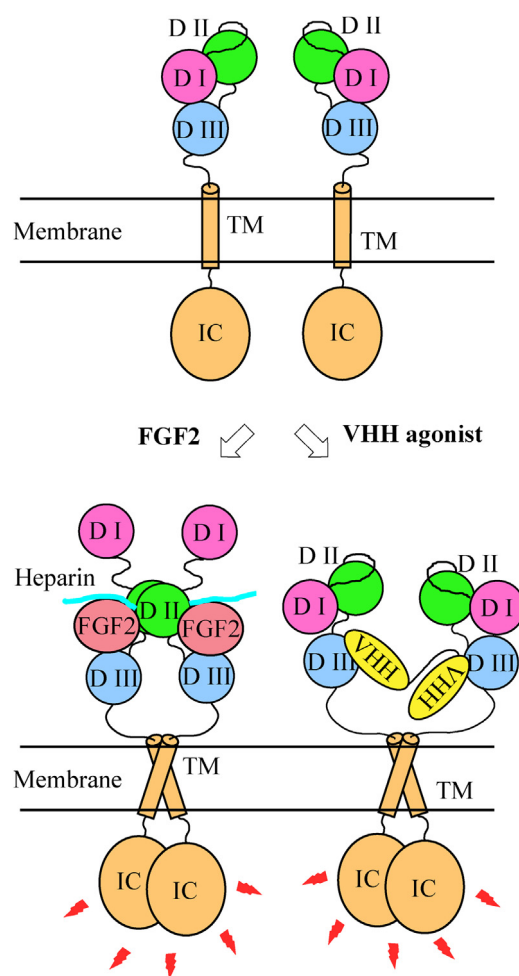


Figure 5. Activation model of FGFR1 by FGF2 or homobivalent agonist VHH. FGFR1 is present in monomeric form under the physiological condition. The D I domain negatively regulates FGF2 binding to the receptor and keeps its inactive form. FGF2 binds to the D II and D III domains with heparin (shown in blue line), introducing the dimerization of FGFR1. The dimerization causes the structural changes of TM and IC domains, resulting in the activation of FGFR1 (left). On the other hand, the homobivalent VHH agonist binds to D III domains and introduces the dimerization of FGFR1. This dimerization could mimic the activated form of FGFR1 at the TM and IC domains (right). FGF2, fibroblast growth factor 2; FGFR1, FGF receptor 1; IC, intracellular; TM, transmembrane; VHH, variable domain of heavy chain of antibody.

subjected to an *in vitro* translation reaction to synthesize mRNA display molecule. The mRNA display molecule was immobilized on streptavidin-coated magnetic beads (SA beads, Dynabeads MyOne Streptavidin C1; Thermo Fisher Scientific, Inc) and reverse transcribed to synthesize the cDNA display molecules. The RNase T1 (Thermo Fisher) was added to release cDNA display molecules. The supernatant containing the cDNA display molecules was collected, and purification was carried out using nickel–nitrilotriacetic acid magnetic beads (His Mag Sepharose Ni; Cytiva).

Affinity selection of VHH binding to FGFR1

The FGFR1β (IIIc)/Fc (R&D Systems) and IgG1 (Fc) Human (R&D Systems) were purchased and biotinylated using a 20-fold molar quantity of EZ-link sulfo NHS-SS Biotin

A novel agonist for FGF receptor 1 functions as FGF2 ligand

(Thermo Fisher) at 25 °C for 30 min and buffer-exchanged by desalting columns (Zeba Spin Desalting Columns; Thermo Fisher). In the initial round of selection, the 100 pmol of biotinylated FGFR1 β (IIIc)/Fc was immobilized on the SA beads. The cDNA display prepared from 192 pmol of mRNA-formed VHH library in 100 μ l of selection buffer was mixed and incubated at 25 °C for 60 min. After four times washing with the selection buffer, the beads were incubated in 40 μ l of selection buffer containing 20 mM Tris(2-carboxyethyl)phosphine at room temperature (RT) for 15 min to elute the binding cDNA display molecules by cleavage of the disulfide bond. The supernatant containing cDNA display molecules was collected. The beads were then further incubated in 10 μ l of 10 mM NaOH at RT for 10 min. The supernatant containing cDNA display molecules was neutralized with 2 μ l of 1 M Tris-HCl (pH 8.0). The above NaOH elution was performed twice. To prepare the cDNA library for the next round of selection, the cDNA attached to the cDNA display was PCR amplified. A total of five rounds of *in vitro* selection was performed according to the aforementioned protocol with minor changes as follows: the cDNA display VHH libraries were prepared from 12 pmol of mRNA in the second round, from 6 pmol in the third round, and from 3 pmol in the fourth and fifth rounds. The biotinylated FGFR1 β (IIIc)/Fc was successively decreased from 100 to 10 pmol. To reduce the background signal, the cDNA display libraries in the second to the fifth rounds were subjected to prescreening with the SA beads immobilized on 100 pmol of biotinylated human IgG1 (Fc) molecules.

Preparation of a phage display VHH library

After the cDNA display selection, the selected VHH genes were PCR amplified using the VHH-specific primers including BamHI and SfiI restriction enzyme sequences. The amplified DNAs encoding VHHs were purified using AMPure XP (Beckman), digested with BamHI and SfiI, and then subcloned into a phagemid vector. The phagemid vector was digested with BamHI and SfiI and purified by agarose gel electrophoresis using FastGene Gel/PCR Extraction Kit (Nippon Genetics Co, Ltd). The purified vector was dephosphorylated using FastAP Thermosensitive Alkaline Phosphatase (Thermo Fisher). The 5- to 10-fold molar quantity VHH DNAs were added to the phagemid vector, ligase was added, and the mixture was incubated at 16 °C for 60 min. The ligation product was ethanol precipitated and electroporated into the *Escherichia coli* TG-1 strain (Lucigen Corp). The culture solution was incubated in a shaker for 30 min at 37 °C for recovery. The culture was streaked out on LB-agar plates and incubated at 30 °C overnight. All colonies on the plates were collected in the culture (candidate mixture) and incubated at 30 °C for 1.5 to 2 h to reach absorbance of 0.5 to 1.0 at 600 nm. The helper phage was added to the culture at 20-fold of the TG-1 quantity and further incubated at 30 °C overnight. The culture was centrifuged at 4000g for 30 min at 4 °C, and the supernatant was collected. The 20% PEG and 2.5 M NaCl solution were added to the supernatant to precipitate the

phages. The mixture was left on ice for 1 h and then centrifuged. The supernatant was removed, and the precipitate dissolved in PBS containing 10% glycerol.

Selection of phage panning for FGFR1 β (IIIc)

One hundred microliters of FGFR1 β (IIIc)/Fc (10 μ g/ml) were added to Immuno Clear Standard Modules (C8, MaxiSorp; Thermo Fisher), and the plate was left overnight at 4 °C. For a negative control, PBS was added to other wells, and the plate was left in the same condition. After washing the wells with PBS three times, PBS containing 3% skim milk was added to each well and incubated at RT for 1 h. Each well was washed with PBS with Tween-20 (PBS-T) four times. Then, 100 μ l of VHH-display phage in PBS containing 1% skim milk and 5% bovine serum albumin (BSA) was added to each well and incubated at RT for 1 h. Each well was washed with PBS-T four times and then shaken with 200 μ l of PBS-T for 5 min. The aforementioned washing step was performed twice under the same conditions. To elute the binding phages, 100 μ l of triethylamine (100 mM) was added to each well and the supernatant collected. Again, 100 μ l of triethylamine (100 mM) was added to each well and incubated at RT for 10 min. All the supernatants were neutralized with 0.5 M Tris-HCl (pH 6.8). The solution was added to 1200 ml of 2-YT with TG-1 and incubated at 30 °C for 1 h. The mixture was centrifuged, and the precipitate containing TG-1 was suspended in the culture medium. The culture was streaked out on LB-agar plates incubated at 30 °C overnight. The VHH-presented phage was prepared according to the aforementioned process, and phage panning was performed again.

Phage ELISA for FGFR1 β (IIIc)

Each round of VHH-display phage was prepared according to the aforementioned procedure. One hundred microliters of FGFR1 β (IIIc)/Fc (10 μ g/ml) was added to Immuno Clear Standard Modules, and the plate was left at 4 °C overnight. After washing with PBS three times, the PBS containing 3% skim milk was added to wells and incubated at RT for 1 h. Each well was washed with PBS-T four times. The 50 μ l of each round of VHH-display phage in PBS, which contained 10% BSA, was added to each well and incubated at RT for 1 h. Each well was washed with PBS-T four times. About 50 μ l of Anti-M13-mAb-horseradish peroxidase in PBS (1/3000 dilution; Sino Biological) was added and incubated at RT for 1 h. After washing with PBS five times, OPD detection reagent (1 tablet in 0.1 M NaH₂PO₄ plus 0.01% H₂O₂; Fujifilm Wako Pure Chemical Corporation) was added to each well and allowed to develop in the dark. After enough color development, 1 M H₂SO₄ was added, and absorbance was measured at 490 nm (reference; 630 nm) using Infinite M Plex (Tecan Group Ltd).

Preparation of monovalent and homobivalent VHHs

Monovalent and homobivalent VHH antibodies were prepared using the *C. glutamicum* expression system Corynex (Ajinomoto Co, Inc). The DNA fragments encoding VHH

antibodies clone VM34 and clone VM35 were inserted into an expression vector using *in vitro* homologous recombination. In the vector, the VHH contains a C-terminal His tag and BamHI site between VHH and the tag. To generate homobivalent VHH antibodies such as VM34-5aa, VM34-10aa, and VM34-20aa, the DNA fragments of monovalent clone VM34 were PCR amplified from the expression vector with linker sequences of GSGGG (5aa), (GSGGG)₂ (10aa), or (GSGGG)₄ (20aa) and two restriction sites, BglII and ApaI. The PCR fragments were then inserted into the clone VM34 expression vector to produce homobivalent VM34-5aa, VM34-10aa, or VM34-20aa. Furthermore, other flexible linkers, GSAG-SAAGSGEF (L3) or GSEKSSGSGSESKST (L4), were introduced instead of the GSGGG linker resulting in VM34-L3 and VM34-L4.

Expression and purification of monovalent and homobivalent VHHs

The resultant expression vectors were introduced into *C. glutamicum*, and the bacterial cells were cultured in CM2G medium at 30 °C overnight. The cells were inoculated in a protein expression medium and cultured at 25 °C for 72 h. The culture supernatants obtained by centrifugation were filtrated through a 0.22- μ m membrane filter and subjected to nickel-nitrilotriacetic acid HP (Fujifilm Wako Pure Chemical Corporation) in a spin column. The resin was washed with a Tris buffer (50 mM Tris-HCl [pH 7.5] and 300 mM NaCl) containing 30 mM imidazole, and the VHH antibodies were then eluted with a Tris buffer containing 500 mM imidazole. The eluate buffer was replaced with PBS using Zeba spin desalting columns (0.5 ml, 7k molecular weight cutoff; Thermo Fisher). The final protein concentrations and their purity were determined by SDS-PAGE and bicinchoninic acid protein assays, respectively.

Thermal stability analysis

The purified VHHs were analyzed for their thermal stability using DSF and SLS assays. A temperature of 1 °C/min was performed with monitoring from 25 to 95 °C. The SLS assays were measured at 266 nm. T_m and T_{agg} from the DSF assay were analyzed and calculated using UNcle Analysis Software (Unchained Labs).

SPR analysis

SPR biosensing experiments were performed on a Biacore T200 using the CAP single-cycle kinetics method (Cytiva) according to Biacore T200 control software. For all measurements, HBS-EP+ (10 mM Hepes, pH 7.4, 150 mM NaCl, 0.5 mM EDTA, 0.05% surfactant P20) was used as the running buffer. Biotinylated recombinant human FGFR1 protein was diluted in HBS-EP+ and immobilized on a Biotin CAPture chip yielding typical levels of approximately 140 RUs. The concentration of samples was injected at 0.62, 1.85, 5.56, 16.67, and 50 nM. The flow rate was 30 μ l/min. The contact and dissociation times were 120 and 600 s, respectively. The dissociation constant was calculated by global fitting of the

concentration series to a 1:1 binding mode using Biacore T200 evaluation software (Cytiva).

Binding competition assay between VM34 and VM35

The binding competition assays between clone VM34 and clone VM35 against the FGFR1 IIIc were performed on a Biacore T200. For all measurements, HBS-EP+ (10 mM Hepes, pH 7.4, 150 mM NaCl, 3 mM EDTA, 0.05% surfactant P20) was used as the running buffer. Biotinylated recombinant human FGFR1-Fc protein was diluted in HBS-EP+ and immobilized on a Biotin CAPture chip. Clone VM35 was injected with 100 nM at a flow rate of 30 μ l/min for 120 s, and subsequent dissociation was followed for up to 30 s. Continuously, clone VM34 was injected with 100 nM for 120 s, and subsequent dissociation was followed for up to 300 s. Data processing and analysis were performed using Biacore T200 evaluation software.

Cell culture of NIH3T3, hMSC, and hiPS

NIH3T3 was purchased from American Type Culture Collection and maintained in Dulbecco's modified Eagle's medium (Sigma-Aldrich, Merck KGaA) supplemented with 10% fetal calf serum (BioWest), penicillin (100 U/ml), and streptomycin (100 μ g/ml) in a humidified 5% CO₂ incubator.

hMSCs from bone marrow were purchased from STEMCELL Technologies and maintained in Dulbecco's modified Eagle's medium (low-glucose; Fujifilm Wako) supplemented with 10% fetal bovine serum (Sigma-Aldrich) in a humidified 5% CO₂ incubator.

The 253G1, the human iPS cell line (6), was purchased from CiRA Foundation and maintained in the complete TeSR-E8 medium (STEMCELL Technologies) supplemented with 10 μ M Y-27632 (Wako Chemicals) on 6-well culture plates coated with iMatrix-511 (Nippi, Incorporated). Cells were incubated at 37 °C in a humidified 5% CO₂ incubator, and the medium was changed daily.

In-cell ELISA for phospho-Erk1/2

The NIH3T3 cells were seeded (10,000 cells per well) on Nunc Edge 96-well plates containing the complete culture medium. After 24 h, the medium was replaced with serum-free culture medium containing FGF2 (100 ng/ml) or VHH candidates, and cells were further incubated for 30 min. Following PBS washes, cells were fixed with 4% paraformaldehyde for 15 min at RT and permeabilized with 0.1% Triton X-100 in PBS for 15 min at RT. The 1% H₂O₂ in PBS was added to each well and left in darkness for 20 min at RT. Following the BSA blocking, cells were incubated overnight at 4 °C with a primary antibody solution (anti-p44/42 MAPK-Erk1/2 rabbit monoclonal antibody, 1/1000 dilution; Cell Signaling Technology). Plates were washed with Tris-buffered saline containing 0.05% Tween-20 three times, and horseradish peroxidase-conjugated anti-rabbit IgG solution (1/1000 dilution; Cell Signaling Technologies) was added and incubated in darkness at RT for 1 h. After final washing, OPD detection reagent (1 tablet in 0.1 M NaH₂PO₄, 0.01% H₂O₂; Fujifilm Wako Pure Chemical

A novel agonist for FGF receptor 1 functions as FGF2 ligand

Corporation) was added to each well, allowed to develop in darkness, and 1 M H₂SO₄ was added to wells. The absorbance was measured at 490 nm (reference: 630 nm) using Infinite M Plex (Tecan). After measuring the absorbance at 490 nm, cells were washed with ultrapure water three times and stained with Janus Green reagent (Abcam) for 5 min at RT. The plate was washed with ultrapure water until excess dye was removed, and 0.5 M HCl was added and incubated for 10 min. The plate was measured at 595 nm using Infinite M Plex (Tecan).

Cell proliferation assay of NIH3T3

The NIH3T3 cells were seeded at a density of 2500 cells per well in white opaque CulturPlate 96-well microplates (PerkinElmer, Inc) containing the complete culture medium. After 24 h, the medium was replaced with serum-free culture medium containing FGF2 (100 ng/ml) or homobivalent VHHs, and cells were further incubated for 48 h. Cell Titer Glo 2.0 reagent (Promega) was added to the wells, and the plate was incubated for 10 min at RT. Luminescence was measured using a Synergy HTX plate reader (BioTek Instruments, Inc).

Determination of hMSC and hiPSC cell growth

To determine the effect of the VHH agonist on cell growth, hMSCs were cultured in the complete culture medium supplemented with bFGF or VHH agonist, and the living cell number was counted using a TC20 automated cell counter (Bio-Rad) on every passage culture.

Human iPSC cells, 253G1s, were cultured with cTeSR-E6 medium (TeSR-E6 medium containing 2 ng/ml transforming growth factor β 1) additionally supplemented with FGF2 or VHH agonist. For the subculture, cells were treated with TrypLE Select (Thermo Fisher Scientific) and dissociated to the single cell. After centrifugation, the cells were resuspended with complete TeSR-E6 medium supplemented with 2 ng/ml transforming growth factor β 1, counted by TC20 automated cell counter, and seeded onto the new 6-well plates. After 24 h subculture, FGF2 or VHH agonist was added to the medium and incubated for 5 to 7 days until 50 to 90% confluent.

Flow cytometry

hMSCs were cultured in CellBIND 6-well plates (Corning) for 5 days and harvested with TrypLE Express (Thermo Fisher Scientific). Collected cell samples were washed with 1% BSA/PBS, resuspended with the antibody solution (CD90; anti-CD90/Thy1 Alexa Fluor488-conjugated antibody, CD105; anti-CD105 PE-conjugated antibody, CD73; anti-CD73 PE-conjugated antibody; R&D Systems) and incubated at 4 °C for 30 min. Following several PBS washes, cells were resuspended with 1% BSA/PBS and then loaded into an Attune NxT Flow Cytometer (Thermo Fisher Scientific).

Differentiation of hMSC to adipocytes or osteocytes

Differentiation to adipocytes or osteocytes was induced by culturing the hMSC in adipogenic differentiation medium or osteogenic differentiation medium (PromoCell) for 2 weeks. Culture medium was refreshed every 4 days. The state of

differentiation was determined by Oil Red staining or Alizarin Red staining.

Immunocytochemistry for undifferentiated state of hiPSCs

After being seeding on 6-well plates, 253G1 cells seeded onto matrix-coated 6-well plate were washed with PBS and fixed with 4% paraformaldehyde in PBS for 30 min at RT. Then, cells were permeabilized with 0.1% Triton X-100 in PBS at RT for 5 min and blocked with 1% BSA/PBS solution at RT for 30 min. To detect OCT4 marker protein, cells were treated with anti-OCT4 rabbit polyclonal antibody as the primary antibody (ab19857; Abcam) and subsequently with Alexa Fluor488-conjugated anti-rabbit IgG antibody (ab150077; Abcam). To detect SSEA4, cells were treated with anti-SSEA4 mouse monoclonal antibody (ab16287; Abcam) as the primary antibody and subsequently with Alexa Fluor647-conjugated antimouse IgG antibody (ab150115; Abcam). The nuclei were stained with 4',6-diamidino-2-phenylindole (Dojindo) in 1% BSA/PBS.

Data availability

All data presented are contained within the article.

Supporting information—This article contains supporting information.

Acknowledgments—We thank Ms Frances Ford for English language review of the article.

Author contributions—R. Y., S. K., K. K., K. W.-N., H. A., Y. U., N. N., and M. T. conceptualization; R. Y., S. K., K. K., K. W.-N., and T. Y. formal analysis; R. Y., S. K., K. K., K. W.-N., M. M., T. M., and T. Y. investigation; A. M. resources; R. Y., S. K., K. K., K. W.-N., N. N., and M. T. writing—original draft; R. Y., N. N., and M. T. writing—review and editing; Y. U. and M. T. supervision; Y. U. and M. T. project administration.

Conflict of interest—The authors declare that they have no conflicts of interest with the contents of this article.

Abbreviations—The abbreviations used are: bFGF, basic fibroblast growth factor; BSA, bovine serum albumin; cDNA, complementary DNA; CDR3, complementarity-determining region 3; DSE, differential scanning fluorimetry; ERK, extracellular signal-regulated protein kinase; ESC, embryonic stem cell; FGF, fibroblast growth factor; FGFR, fibroblast growth factor receptor; FGFR1 ED, FGFR1 extracellular domain; hiPSC, human-induced pluripotent stem cell; hMSC, human mesenchymal stem cell; IC, intracellular; IgG, immunoglobulin G; MAPK, mitogen-activated protein kinase; PBS-T, PBS with Tween-20; PSC, pluripotent stem cell; RT, room temperature; SLS, static light scattering; SPR, surface plasmon resonance; VHH, variable domain of heavy chain of heavy chain antibody.

References

1. Xie, Y., Su, N., Yang, J., Tan, Q., Huang, S., Jin, M., et al. (2020) FGF/FGFR signaling in health and disease. *Signal Transduct. Target. Ther.* 5, 181

- Huang, Y., Hamana, T., Liu, J., Wang, C., An, L., You, P., *et al.* (2015) Type 2 fibroblast growth factor receptor signaling preserves stemness and prevents differentiation of prostate stem cells from the basal compartment. *J. Biol. Chem.* **290**, 17753–17761
- Tian, R., Yao, C., Yang, C., Zhu, Z., Li, C., Zhi, E., *et al.* (2019) Fibroblast growth factor-5 promotes spermatogonial stem cell proliferation via ERK and AKT activation. *Stem Cell Res. Ther.* **10**, 40
- Mossahebi-Mohammadi, M., Quan, M., Zhang, J. S., and Li, X. (2020) FGF signaling pathway: a key regulator of stem cell pluripotency. *Front. Cell Dev. Biol.* **8**, 79
- Mayes, P. A., Hance, K. W., and Hoos, A. (2018) The promise and challenges of immune agonist antibody development in cancer. *Nat. Rev. Drug Discov.* **17**, 509–527
- Nakagawa, M., Koyanagi, M., Tanabe, K., Takahashi, K., Ichisaka, T., Aoi, T., *et al.* (2008) Generation of induced pluripotent stem cells without Myc from mouse and human fibroblasts. *Nat. Biotechnol.* **26**, 101–106
- Nakashima, Y., and Omasa, T. (2016) What kind of signaling maintains pluripotency and viability in human-induced pluripotent stem cells cultured on laminin-511 with serum-free medium? *Biores. Open Access* **5**, 84–93
- Hui, Q., Jin, Z., Li, X., Liu, C., and Wang, X. (2018) FGF family: from drug development to clinical application. *Int. J. Mol. Sci.* **19**, 1875
- Ueki, R., Atsuta, S., Ueki, A., Hoshiyama, J., Li, J., Hayashi, Y., *et al.* (2019) DNA aptamer assemblies as fibroblast growth factor mimics and their application in stem cell culture. *Chem. Commun.* **55**, 2672–2675
- Hoey, R. J., Eom, H., and Horn, J. R. (2019) Structure and development of single domain antibodies as modules for therapeutics and diagnostics. *Exp. Biol. Med. (Maywood)* **244**, 1568–1576
- Yamaguchi, J., Naimuddin, M., Biyani, M., Sasaki, T., Machida, M., Kubo, T., *et al.* (2009) cDNA display: a novel screening method for functional disulfide-rich peptides by solid-phase synthesis and stabilization of mRNA-protein fusions. *Nucleic Acids Res.* **37**, e108
- Ueno, S., Yoshida, S., Mondal, A., Nishina, K., Koyama, M., Sakata, I., *et al.* (2012) *In vitro* selection of a peptide antagonist of growth hormone secretagogue receptor using cDNA display. *Proc. Natl. Acad. Sci. U. S. A.* **109**, 11121–11126
- Mochizuki, Y., Nishigaki, K., and Nemoto, N. (2014) Amino group binding peptide aptamers with double disulphide-bridged loops selected by *in vitro* selection using cDNA display. *Chem. Commun.* **50**, 5608–5610
- Kobayashi, S., Terai, T., Yoshikawa, Y., Ohkawa, R., Ebihara, M., Hayashi, M., *et al.* (2017) *In vitro* selection of random peptides against artificial lipid bilayers: a potential tool to immobilize molecules on membranes. *Chem. Commun.* **53**, 3458–3461
- Jayathilake, C., Kumachi, S., Arai, H., Motohashi, M., Terai, T., Murakami, A., *et al.* (2020) *In vitro* selection of anti-gliadin single-domain antibodies from a naive library for cDNA-display mediated immuno-PCR. *Anal. Biochem.* **589**, 113490
- Decker, C. G., Wang, Y., Paluck, S. J., Shen, L., Loo, J. A., Levine, A. J., *et al.* (2016) Fibroblast growth factor 2 dimer with superagonist *in vitro* activity improves granulation tissue formation during wound healing. *Biomaterials* **81**, 157–168
- Ballinger, M. D., Shyamala, V., Forrest, L. D., Deuter-Reinhard, M., Doyle, L. V., Wang, J. X., *et al.* (1999) Semirational design of a potent, artificial agonist of fibroblast growth factor receptors. *Nat. Biotechnol.* **17**, 1199–1204
- Schlessinger, J., Plotnikov, A. N., Ibrahimi, O. A., Eliseenkova, A. V., Yeh, B. K., Yayon, A., *et al.* (2000) Crystal structure of a ternary FGF-FGFR-heparin complex reveals a dual role for heparin in FGFR binding and dimerization. *Mol. Cell* **6**, 743–750
- Sarabipour, S., and Hristova, K. (2016) Mechanism of FGF receptor dimerization and activation. *Nat. Commun.* **7**, 10262
- Yoshimura, Y., and Fujimoto, K. (2008) Ultrafast reversible photo-cross-linking reaction: toward *in situ* DNA manipulation. *Org. Lett.* **10**, 3227–3230